Lu Yangfang
Wang Hui
Xue Yun
Gu Xue
Wang Yan
Yan Chao

School of Pharmacy, Shanghai Jiao Tong University, Shanghai, Shanghai, P. R. China

Received March 5, 2015
Revised April 20, 2015
Accepted April 27, 2015

Research Article

Preparation and evaluation of monodispersed, submicron, non-porous silica particles functionalized with β-CD derivatives for chiral-pressurized capillary electrochromatography

Submicron, non-porous, chiral silica stationary phase has been prepared by the immobilization of functionalized β-CD derivatives to isocyanate-modified silica via chemical reaction and applied to the pressurized capillary electrochromatography (pCEC) enantio-separation of various chiral compounds. The submicron, non-porous, cyclodextrin-based chiral stationary phases (sub_μm-CSP2) exhibited excellent chiral recognition of a wide range of analytes including clenbuterol hydrochloride, mexiletine hydrochloride, chlorpheniramine maleate, esmolol hydrochloride, and metoprolol tartrate. The synthesized submicron particles were regularly spherical and uniformly non-porous with an average diameter of around 800 nm and a mean pore size of less than 2 nm. The synthesized chiral stationary phase was packed into 10 cm × 100 μm id capillary columns. The sub_μm-CSP2 column used in the pCEC system showed better separation of the racemates and at a higher rate compared to those used in the capillary liquid chromatography mode (cLC) system. The sub_μm-CSP2 possessed high mechanical strength, high stereoselectivity, and long lifespan, demonstrating rapid enantio-separation and good resolution of samples. The column provided an efficiency of up to 170 000 plates/m for *n*-propylbenzene.

Keywords:
β-CD / Chiral separation / cLC / pCEC / Submicron non-porous chiral stationary phase
DOI 10.1002/elps.201500122

1 Introduction

In LC, according to van Deemter equation, the lower the stationary phase particle size, the higher the separation column efficiency and faster analysis speed. In recent years, particle sizes ranging from 1.7 to 2.0 μm have been successfully used in commercial products. Conventional LC does not allow for the application of smaller particles (nano or submicron) because of the pressure limitations of commercially available pumping systems [1]. Jerkovich et al. found that the column backpressure could reach 55.16 Mpa when the stationary phase particle size decreased to 1.5 μm [2]. The emergence of ultra-high performance liquid chromatography (UPLC) brought about a silver lining to this problem. Another way to solve the high backpressure problem is by the application of CEC in which the mobile phase is driven by EOF [3], but bubble formation caused by the Joule-heating effect occurs when high voltage is applied.

Pressurized capillary electrochromatography (pCEC) is the hybrid of HPLC and CEC, offering high column efficiency, short analysis time, and low consumption of analytes and solvent. According to the varying partition coefficients and electrophoretic migration in the electric field, samples are separated by pCEC [4–6]. This micro-separation technique has developed rapidly as an alternative to traditional HPLC, and when using the submicron particles, reasonable linear velocity was achieved by using low pressure [7].

Enantiomeric forms of a drug can differ in potency, toxicity, and behavior in biological systems [8]. At present, the diameters of most commercial liquid chromatographic chiral packings are 3, 5, and 10 μm. A great deal of research has been conducted on the application of chromatographic packings with diameters ranging between 1 and 2 μm [1, 9–16]. Wang et al. reviewed the applications of sub_2 μm materials in LC [17]. Chiral silica particles between 1 and 2 μm were also studied by research groups recently [18–23].

Correspondence: Dr. Wang Yan, **E-mail:** wangyan11@sjtu.edu.cn
Dr. Yan Chao, **E-mail:** chaoyan@unimicrotech.com.

Abbreviations: cLC, capillary liquid chromatography; **CSP**, chiral stationary phase; **pCEC**, pressurized capillary electrochromatography; **UPLC**, ultra-high performance liquid chromatography

Colour Online: See the article online to view Fig. 4 in colour.

The application of submicron chiral chromatography is not very common. Most studies on the application of submicron silica in chiral chromatography have focused on CEC [24–26]. Fanali's group prepared different chiral stationary phases (CSPs), such as amylose tris(5-chloro-2-methylphenylcarbamate) based [27], cellulose tris(4-chloro-3-methylphenylcarbamate) based [28], and so on, and then achieved good separation of racemates in CEC mode. Chankvetadze's group also studied several CSPs in nano-LC and CEC mode, and better peak efficiencies and resolution were observed by using CEC experiments compared to nano-LC mode [29]. Ai's group prepared 600–900 nm of meso-porous β-CD bonded silica particles and achieved well separated racemates in UPLC mode [30]. Li's group prepared 500–800 nm of meso-porous β-CD bonded silica particles in CEC mode, and a variety of enantiomers were baseline separated [31]. Lin's group applied 5 μm of particles functionalized with β-CD derivatives to pCEC system and achieved fast separation of propranolol [32]. To the best of our knowledge, the submicron, non-porous chiral packing in the application of pCEC has not been previously reported in the literature.

This study is the first demonstration of enantioseparation of five racemates using submicron, non-porous silica CSPs in pCEC mode. Non-porous silica particles measuring 800 nm were prepared by using a modified Stöber method. The β-CD derivatives were chemically linked to submicron, non-porous silica particles via a 3-(triethoxysilyl) propyl isocyanate coupling agent. With the active functional group (NCO), 3-(triethoxysilyl) propyl isocyanate was chosen to improve β-CD coverage in our preparation route, which differed from references [30, 31]. With the drive of electroosmotic and pressure flow, four groups of positional isomers and five racemates were baseline separated.

2 Materials and methods

2.1 Chemicals and materials

β-Cyclodextrin (β-CD), tetraethoxysilane (TEOS), ammonium hydroxide (25% to 28%), benzene (99.8%), methylbenzene (anhydrous, 99.8%), ammonium acetate (≥98%), and pyridine (anhydrous, 99.8%) were obtained from Sinopharm Chemical Reagent Company (Shanghai, China). 3-(triethoxysilyl) propyl isocyanate (95%), phenyl isocyanate (98%), ethylbenzene (≥98%), propylbenzene (≥98%), and *n*-butyl benzene (≥98%), and all chiral analytes were purchased from Aladdin (Shanghai, China), Ai Keda Chemical Technology (Chengdu, China), and National Institutes for Food and Drug Control (Beijing, China), respectively. HPLC-grade acetonitrile (ACN) and methanol (MeOH) were obtained from TEDIA (OH, USA) and used directly. The water used was MilliQ grade (Millipore, Bedford, MA, USA).

2.2 Preparation of submicron, non-porous chiral stationary phase (sub_μm-CSP2)

Non-porous submicrometer-sized silica spheres were synthesized using modified Stöber method according to the literature [7]. Briefly, TEOS (0.25 mol/L), ethanol (6%), and ammonia (3.0 mol/L) were dissolved in water, and the mixture was kept at room temperature for 16 h with stirring. After 12 h, a white powder was collected and washed with water and ethanol. Then, hydrochloric acid (3 mol/L) was added, and the solution was stirred at room temperature for another 12 h. The solid phase was washed with water and then dried in a vacuum at 60°C.

A mixture consisting of 2 g of β-CD and 0.6 mL of 3-(triethoxysilyl) propyl isocyanate was dissolved in 30 mL anhydrous pyridine and stirred at 80°C for 12 h under an inert atmosphere of nitrogen gas. Anhydrous pyridine (10 mL) and 0.6 g of silica particles were added, and the solution was stirred continuously for 20 h at 100°C with N_2 protection. The product, sub_μm-CSP1, was washed with anhydrous pyridine, anhydrous toluene, MeOH, and anhydrous diethyl ether, and then dried in a vacuum at 60°C. sub_μm-CSP1 (0.4 g) was dispersed in 30 mL of anhydrous pyridine, and 2 mL of phenyl isocyanate was added. Then, the reaction mixture was stirred for 12 h at 90°C. After cooling to room temperature, the obtained sub_μm-CSP2 was washed with anhydrous pyridine, anhydrous toluene, MeOH, water, and anhydrous diethyl ether, and then dried in a vacuum at 60°C.

2.3 Preparation of packed capillaries

The chiral column was packed through a slurry packing procedure as follows: 0.05 g of sub_μm-CSP2 (800 nm) was dispersed in 1 mL anhydrous ethanol. The slurry was packed into the capillary under 5000 psi, and then the pressure was increased slowly to 9000 psi. After that, ethanol was exchanged for water, and the column sat under 9000 psi for 2 h. After preparing the middle frit, the initial frit was cut and the detection window was prepared near the middle frit. The initial and middle frits were prepared with an electrical heating unit (600–900°C, 15 s). The total length of column obtained was 400 mm (effective length was 100 mm).

2.4 Characterization

SEM images were obtained on an S-4800 field emission scanning electron microscope (Hitachi, Japan) with an accelerating voltage of 10 kV. FTIR analysis was performed on a Nicolet 6700 Fourier transform infrared spectrometer (Thermo Nicolet Corp., Madison, WI, USA) to determine the C, H, and N contents of the synthesized sub_μm-CSP2. Elemental analysis experiments were undertaken on Vario EL Cube Elemental Analysis (Elementar, Germany). Nitrogen

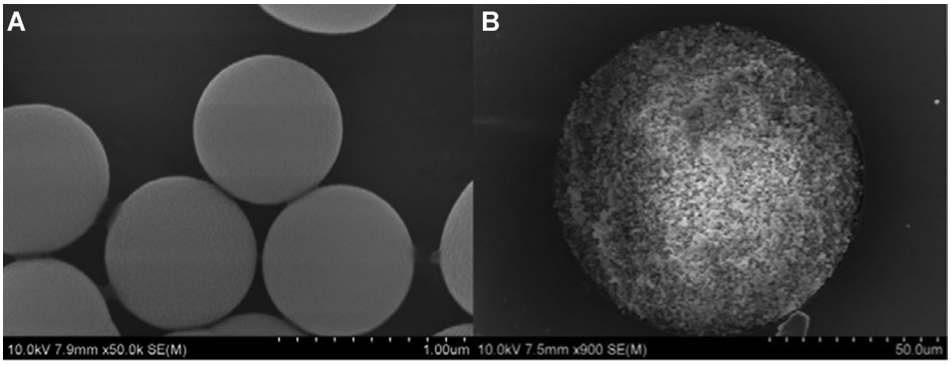

Figure 1. SEM image of submicron SiO_2 particles (A) and razor blade-cut section of 100 μm id capillary column (B).

physisorption isotherms were measured using a Quantachrome Autosorb 1C apparatus at 196°C. Prior to all measurements, the samples were de-gassed under vacuum at 150°C for 10 h. Brunauer–Emmett–Teller (BET) surface areas were calculated from data on adsorption at a relative pressure range between 0.04 and 0.25. Thermal analysis (TGA) was conducted on a Pyris 1 TGA Thermo Gravimetric Analyzer (PerkinElmer Shelton, CT, USA) with a heating rate of 10°C/min from 0 to 900°C under nitrogen. In the preparation of the capillary column, the initial and middle frits were prepared with an electrical heating unit (Unimicro Technologies, Inc., Pleasanton, CA, USA).

2.5 pCEC operations

The pCEC system used for the chromatographic test was TriSep-2100GV (Unimicro Technologies, Inc., Pleasanton, CA, USA). It is possible to perform pCEC, capillary LC (cLC), and CE independently on the same system. All the buffers were prepared by dissolving ammonium acetate in ultra-pure water and adjusting to the desired pH with acetic acid or ammonia. The mobile phase consisted of a mixture of ACN with hydrochloric acid and acetic acid-ammonium acetate buffer solution (5 mmol/L, pH 4.0) unless otherwise indicated. Samples were prepared by dissolving analytes in mobile phase with concentrations of 1 mg/mL and diluting them to the desired concentrations before use. All samples and mobile phase were filtered before use. Applied voltage ranged from 0 to 12 kV, and the flow rate of pump ranged from 0.03 mL/min to 0.06 mL/min. All experiments were carried out at room temperature.

3 Results and discussion

3.1 Synthesis of sub_μm-CSP2

The simplest way to synthesize spherically-shaped silica is by using the Stöber method [33]. With this procedure, spheres can be synthesized into a large number of sizes by controlling the pH conditions in the synthetic environment [34]. In this study, non-porous, submicron silica particles were prepared by a modified Stöber method. The SEM image of the synthesized 800 nm silica spheres indicated that the silica particles were very homogeneous in their particle size at a micro-structural level (Fig. 1A). The surface area of silica particles was 15 m^2/g with a mean pore size of less than 2 nm, tested by BET method which was consistent with the literature [7].

The first successful high coverage and stable CD-bonded CSP was developed by Armstrong using epoxide ether linkages [35]. There are many methods for surface modification of silica. General silane coupling agents include 3-(mercaptopropyl) trimethoxysilane [31], γ-(2, 3-epoxypropoxy) propyltrimethoxysilane [36], aminopropyltriethoxysilane [37], 3-(triethoxysilyl) propyl isocyanate [38], etc. Here, 3-(triethoxysilyl) propyl isocyanate was selected as a coupling agent because of its active functional group (NCO). To the best of our knowledge, 3-(triethoxysilyl) propyl isocyanate in the preparation of submicron non-porous chiral packing has not been previously reported in the literature. This route was simple but effective, and β-CD and silica particles were connected by two steps.

3.2 Characterization of sub_μm-CSP2

SEM image of cross section: The column bed was formed with the uniform submicron silica spheres (Fig. 1B). The image illustrated that submicron, non-porous silica particles were packed in a close arrangement. Submicron-sized particles and high stacking density make for better separation ability, higher column efficiency, and better mechanical strength. Moreover, faster analysis speed can also be obtained due to the distinctive non-porous structure.

FTIR analysis of sub_μm-CSP2: The absorption band at 2933, 2865 cm^{-1} are assigned to the -CH_2- group. The -NH- absorption peak at 3600 cm^{-1} was also observed. The changes at 1157 and 1091 cm^{-1} also suggest that β-CD derivatives were successfully bonded.

Elemental analysis of sub_μm-CSP2: the results showed that the carbon content was 2.99% and hydrogen was 1.33%. Meanwhile, nitrogen content was less than 0.3%. The

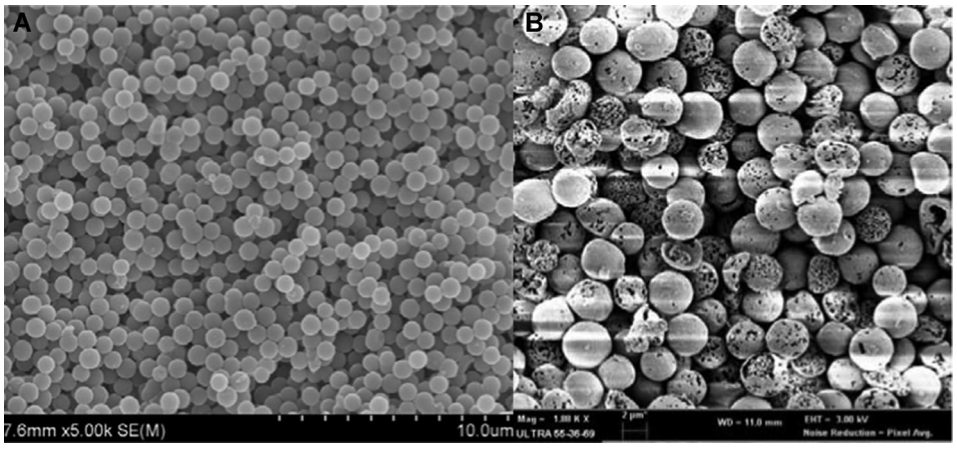

Figure 2. SEM image of sub_μm-CSP2 column (A) and conventional 3 μm porous column (B) after 400 injections of sample.

estimated β-CD loading was 86.52 × 10^{-8} mol/m^2 according to Eq. 1 [39]. The CD coverage was much higher than the submicron porous chiral silica particles (16.36 × 10^{-8} mol/m^2) [31] and 3 μm porous chiral silica particles (15.60 × 10^{-8} mol/m^2) [31].

$$(\mu\text{mol/m}^2) = \frac{\%C \times 10^6}{12 \times N_C \times S} \quad (1)$$

(where % *C* is the carbon content, N_C is the carbon number, and *S* is the surface area of silica particles).

Thermal analysis of sub_μm-CSP2: the grafting ratio determined by TGA method is not shown here. Two main decomposition steps can be observed. The first weight loss occurred below 100°C, assigned to dehydration of water. The second weight loss at about 300°C was assigned to the decomposition of β-CD derivatives, mainly carbohydrates. The total weight loss percentage for samples was 12%. Removing the moisture factors, weight loss percentages for samples was 6%, which was consistent with the β-CD loading described above. The results also suggested that β-CD was successfully introduced onto the surface of sub_μm-CSP2.

Molish Reaction of sub_μm-CSP2: β-CD is a cyclic oligosaccharide which consists of seven glucose units. In the presence of concentrated sulfuric acid, β-CD can produce furfural and its derivatives, which can form red–purple complexes when confronted with α-naphthol. In this test, Molish Reaction of sub_μm-CSP2 was positive. These results support immobilization of β-CD derivatives onto the silica.

Assessment of lifespan: the synthesized sub_μm-CSP2 has better mechanical strength and longer service life because of the non-porous structural quality. After 400 times of sample injection, the cross section SEM image of sub_μm-CSP2 column illustrated that particles had no obvious damage (Fig. 2A). However, with the same conditions, the conventional 3 μm porous packings showed obvious damage (Fig. 2B) in our previous study. For the foreseeable future, submicron silica particles will be more popular. The longer service life of sub_μm non-porous packings will be a great advantage compared to the conventional 3 μm porous packings.

3.3 Separation of positional isomers

Molecular structures of positional isomers are different, so they can be separated more easily than racemates on a chiral column. cLC mode only uses pressure-driven flow. Obviously, its selectivity is not as high as pCEC mode. In cLC mode, the sub_μm-CSP2 was evaluated for separation of four groups of positional isomers. As shown in Fig. 3, those positive separation results showed that the sub_μm-CSP2 embodied fine stereo-selectivity towards positional isomers with simple binary mobile phase. Ortho isomers can produce hydrogen bonds easily. With high hydrophobicity, the ortho isomer was finally eluted (pyrocatechol). The retention time of *o*-nitroaniline was shorter than *p*-nitroaniline, because the molecule structure of *p*-nitroaniline is linear. It can, therefore, enter the β-CD cavity easily and deeply. At this time, large cylindrical cavities of β-CD play an important role. These results suggest that resolution with CD-derived sub_μm CSP2 depend on a complex interplay of host-guest inclusion, hydrogen bonding, π-π conjugate effect, and hydrophobicity.

3.4 Enantio-separation of pharmaceutical compounds

3.4.1 Effect of organic modifier on enantio-separation

In RP mode, mobile phase usually consists of buffer salt solution and organic modifier. Different organic modifiers have different selectivity. The choice of an appropriate organic modifier for certain analytes is an important consideration for separation method development and optimization. An ammonium acetate buffer concentration of 5 mmol/L was fixed as the optimum concentration. The effect of the organic modifier was investigated with MeOH and ACN. The sub_μm-CSP2 column with ACN showed better separation and faster speed compared to those with MeOH. This phenomenon was consistent with past research [40]. This could

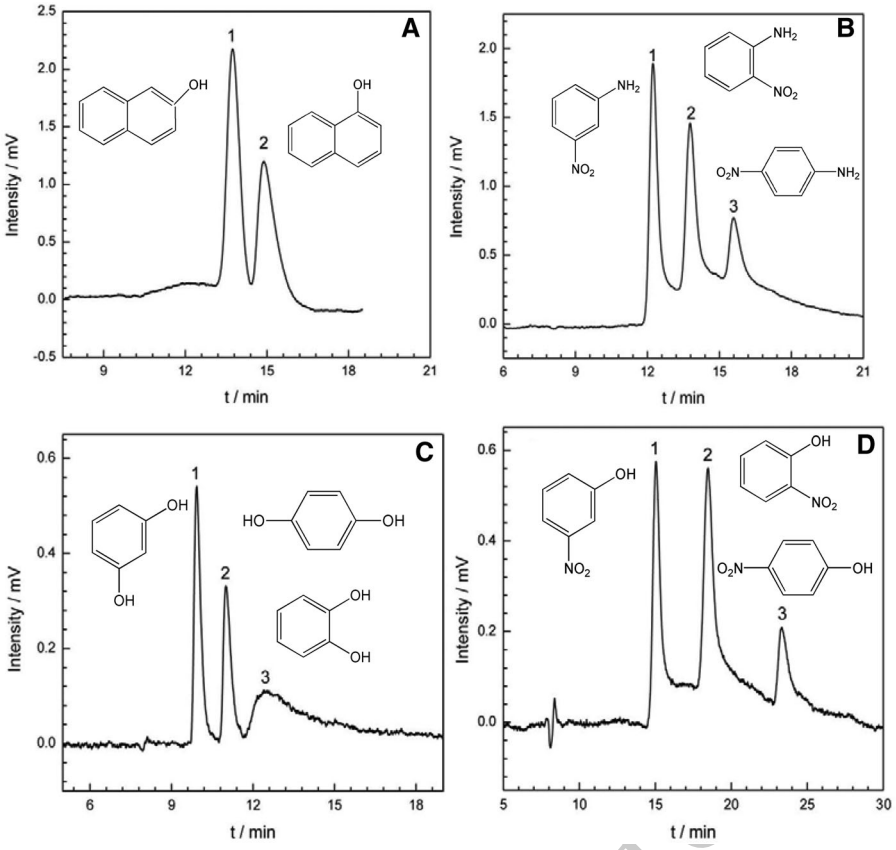

Figure 3. Chromatogram of positional isomers on sub_μm-CSP2 column. Conditions: cLC mode; column dimension: 100 mm (total length 400 mm) ×100 μm id; mobile phase: (A) ACN/ H_2O (40/60, v/v), (B) ACN/ H_2O (40/60, v/v), (C) ACN/ H_2O (20/80, v/v), (D) ACN/ H_2O (40/60, v/v), pump flow rate: 0.05 mL/min. Peak identification: (A) 1. β-naphthol, 2. α-naphthol; (B) 1. *m*-nitroaniline, 2. *o*-nitroaniline, 3. *p*-nitroaniline; (C) 1. Hydroquinone, 2. resorcinol, 3. Pyrocatechol; (D) 1. *m*-nitrophenol, 2. *o*-nitrophenol, 3. *p*-nitrophenol.

Table 1. Effect of ACN concentration and applied voltage on resolution of sub_μm-CSP2 column

Samples	Resolution (Rs)											
	ACN concentration in mobile phase (%)							Applied voltage (kV)				
	10	20	30	40	50	70	90	0	3	6	9	12
1	1.85	2.01	1.69	1.3	1.12	0.56	0	2.11	2.10	2.19	1.40	0.96
2	1.36	1.37	1.47	1.28	0.92	0	0	1.53	1.54	2.32	1.32	0.83
3	1.63	1.68	1.53	1.39	0.98	0	0	1.68	1.7	1.46	1.34	1.12
4	1.53	1.62	1.8	1.43	1.02	0	0	1.80	1.82	1.5	1.28	0.87
5	1.37	1.4	1.47	1.36	0.87	0	0	1.47	1.53	1.36	1.17	0.79

be due to the stronger elution capability and lower viscosity of ACN. Moreover, for UV detection, the methanol cut-off wavelength is 210 nm, but the ACN cut-off wavelength is 190 nm. ACN was eventually chosen.

3.4.2 Effect of ACN concentration on resolution

The effects of ACN concentration on resolution were investigated in the range between 10 and 90% (Table 1). As ACN concentration increased, the resolution of five racemates increased at first and then dropped. This could be due to the lower polarity of ACN which affords a higher probability to compete with the analytes in occupying the CD hydrophobic cavity. Samples 1–5 in Table 1 are (±) clenbuterol hydrochloride, (±) mexiletine hydrochloride, (±) chlorpheniramine maleate, (±) esmolol hydrochloride, and (±) metoprolol tartrate, respectively.

3.4.3 Effect of pH and concentration of ammonium acetate buffer on resolution

Acetic acid–ammonium acetate buffer solution was selected as the buffer salt solution in this study. To investigate the effect of pH on resolution, the pH of the mobile phase was

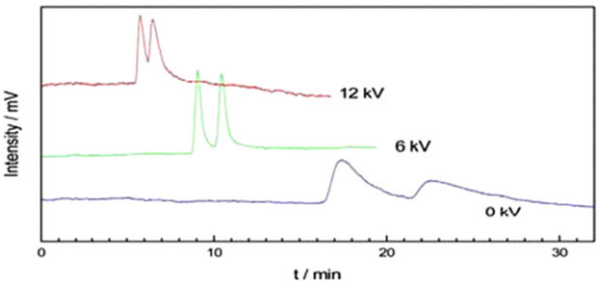

Figure 4. Chromatogram of clenbuterol hydrochloride with various applied voltages. Conditions: pCEC mode; column dimension: 100 mm (total length 400 mm) × 100 μm id; mobile phase: ACN/ H_2O (20/80, v/v) containing 5 mmol/L ammonium acetate, pH 4.0; pump flow rate: 0.05 mL/min; applied voltage: 0–12 kV. Sample: (±) clenbuterol hydrochloride.

gradually increased from 3.0 to 8.0. It was found that good separation could be achieved when the pH was 4.0. A possible explanation is that five basic drugs were in the best state of ionization when pH was 4.0 and could occupy the β-CD hydrophobic cavity easily.

Besides the influence of buffer pH, the effect of ammonium acetate concentration was also investigated in this study. The pH value and proportion of buffer solution was fixed at optimum conditions, and the ammonium acetate concentration ranging from 5 to 40 mmol/L was tested. From 5 to 10 mmol/L, the resolution changed little. As the concentration increased, it was observed that a concentration higher than 10 mmol/L produced a decrease in resolution and peak areas. Considering the electrical test of follow-up experiments, a concentration of 5 mmol/L was finally recommended.

3.4.4 Effect of voltage on enantio-separation

The migration behavior of racemates was influenced by pressure-driven flow, EOF, and electrophoresis. Since EOF was from anode to cathode [41], the directions of EOF, pressure-driven flow, and electrophoresis were in the same direction when negative voltage was applied to the capillary outlet end (negative polarity mode) and the inlet end was grounded, which allowed for faster separation in contrast to cLC. However, when positive voltage was applied to the outlet end (positive polarity mode), the direction of pressure-driven flow was opposite that of EOF and electrophoretic migration, which led to slower elution rates. In this study, negative voltage was selected. When the voltage increased from 0 to12 kV, the resolution of five racemates increased

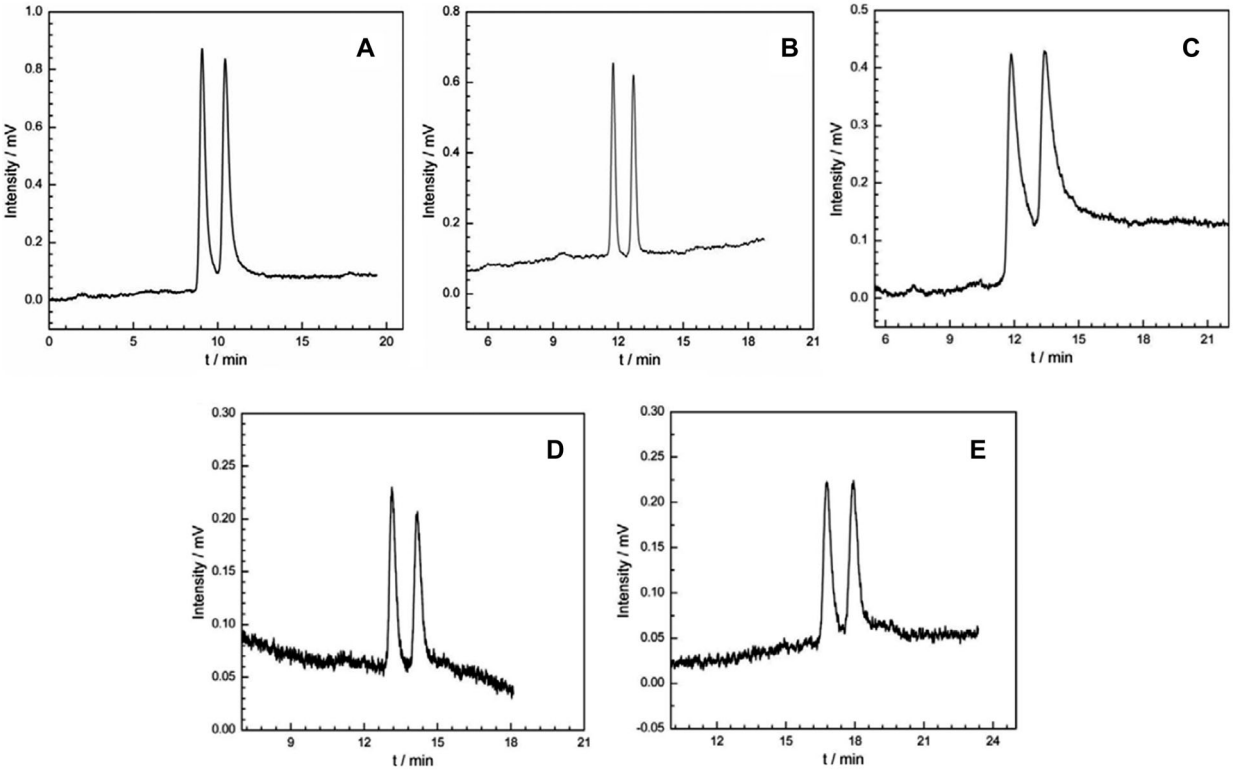

Figure 5. Chromatogram of racemates on sub_μm-CSP2 column. Conditions: pCEC mode; column dimension: 100 mm (total length 400 mm) × 100 μm; mobile phase: (A) ACN/ H_2O (20/80, v/v) containing 5 mmol/L ammonium acetate, pH 4.0, applied voltage 6 kV, pump flow rate: 0.05 mL/min; (B) ACN/ H_2O (30/70, v/v) containing 5 mmol/L ammonium acetate, pH 4.0, applied voltage 6 kV, pump flow rate: 0.05 mL/min; (C) ACN/ H_2O (20/80, v/v) containing 5 mmol/L ammonium acetate, pH 4.0, applied voltage 3 kV, pump flow rate: 0.05 mL/min, splitting ratio was about 300:1; mobile phase for the compounds (D) and (E): ACN/ H_2O (30/70, v/v) containing 5 mmol/L ammonium acetate, pH 4.0, applied voltage 3 kV, pump flow rate: 0.05 mL/min. Samples: (A) (±) clenbuterol hydrochloride; (B) (±) mexiletine hydrochloride; (C) (±) chlorpheniramine maleate; (D) (±) esmolol hydrochloride; (E) (±) metoprolol tartrate.

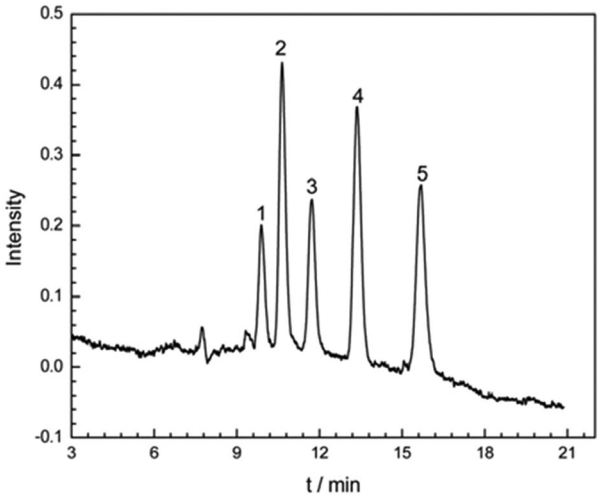

Figure 6. Chromatogram of benzene series on sub_μm-CSP2 column. Conditions: cLC mode; column dimension: 100 mm (total length 400 mm) × 100 μm id; mobile phase: ACN/ H_2O (50/50, v/v), pump flow rate: 0.05 mL/min; linear velocity: 0.3 mm/s; peak identification: (1) benzene; (2) toluene; (3) ethylbenzene; (4) phenylpropane; (5) *n*-butyl benzene.

at the beginning, then dropped (Table 1). Distinctly different peaks of clenbuterol hydrochloride were observed in Fig. 4. As can be seen from Fig. 4, the peaks of chiral compounds have significantly improved with the increase of applied voltage because EOF produces a plug-like flow profile, while the pressure-driven flow produces a parabolic flow profile. At higher voltage, Joule-heating may be dominant, resulting in peak broadening in the capillary column without cooling.

3.4.5 Separation of five basic chiral drugs

With the analyzing condition optimized, the ideal analyzing condition of organic modifier, ACN concentration, pH value, concentration of buffer, and applied voltage were defined. Five racemates were baseline separated in the best conditions. Resolutions were 2.19, 2.32, 1.70, 1.80, and 1.53, respectively. The chromatograms are shown in Fig. 5.

3.5 Reverse-phase chromatographic performance

Reverse-phase chromatographic performance was evaluated with a benzene series in cLC mode. Hydrophobicity, which relates to the number of methylene groups in molecular structure, was investigated using benzene, toluene, ethylbenzene, phenylpropane, and *n*-butyl benzene. As seen from the order of the peaks (Fig. 6), *n*-butyl benzene had the longest retention time for its high hydrophobicity. In the separation of non-polar compounds, sub_μm-CSP2 showed a typically weak reverse-phase chromatographic performance, which resulted from the benzene ring and methylene group in sub_μm-CSP2. Besides enantiomeric recognition and separation potency, sub_μm-CSP2 also has reverse-phase chromatographic performance and could be applied to the analysis of some non-polar or weak-polar substances. Additionally, the sub_μm-CSP2 column provided an efficiency of up to 170 000 plates m^{-1} in the separation of the benzene series.

4 Concluding remarks

A novel 800 nm non-porous, cyclodextrin chiral stationary phase (sub_μm-CSP2) was synthesized with surface loading of 86.52×10^{-8} mol/m^2. Successful enantio-separations of various positional isomers and somew racemates were achieved on the sub_μm-CSP2 column in both the cLC and pCEC modes. Besides enantiomeric recognition and separation potency, the sub_μm-CSP2 also had reverse-phase chromatographic capability and could be applied to the analysis of some non-polar or weak-polar substances. sub_μm-CSP2 has better mechanical strength and a longer lifespan compared to the traditional 3 μm porous chromatographic packings. The experimental results showed that the chromatographic peak in the pCEC system was better than that of the cLC system due to the addition of electroosmotic drive. Additionally, with the drive of electroosmotic and pressure flow, the resolution was improved compared to the pure-pressure driven flow. Therefore, the application of submicron non-porous silica particles in pCEC is feasible. The sub_μm-CSP2 column provided an efficiency of up to 170 000 plates/m for *n*-propylbenzene, 120 000 plates/m for clenbuterol hydrochloride, and 150 000 plates/m for mexiletine hydrochloride.

This work was supported by the National Natural Science Foundation of China (21105064 and 21175092), a specially funded program on the development of national key scientific instruments and equipment (2011YQ150072, 2011YQ15007204, 2011YQ15007207, 2011YQ15007210), and the Natural Science Foundation of Shanghai (12ZR1413600).

The authors have declared no conflict of interest

5 References

[1] Gong, Y., Xiang, Y., Yue, B., Xue, G., Bradshaw, J. S., Lee, H. K., Lee, M. L., *J. Chromatogr. A* 2003, *1002*, 63–70.

[2] Jerkovich, A. D., James, J. S. M., Jorgenson,W., *LC GC N. Am.* 2003, *21*, 600–611.

[3] Zhang, X., Wang, Y., Gu, X., Qu, Q., Yan, C., *Chin. J. Anal. Chem.* 2011, *39*, 455–460.

[4] Zhang, H., Wang, Y., Gu, X., Zhou, J., Yan, C., *Electrophoresis* 2011, *32*, 340–347.

[5] Wu, Y., Wang, Y., Gu, X., Zhang, L., Yan, C., *J. Sep. Sci.* 2011, *34*, 1027–1034.

[6] Yan, R. H., Gao, Y., Wang, X., Zhang, X., Yan, C., Wang, Y., *J. Chromatogr. Sci.* 2012, *00*, 1–3.

[7] Qu, Q., Lu, X., Huang, X., Hu, X., Zhang, Y., Yan, C., *Electrophoresis* 2006, *27*, 3981–3987.

[8] Kragh-Hansen, U., Chuang, V. T. G., Otagiri, M., *Biol. Pharm. Bull.* 2002, *25*, 695–704.

[9] Wan, H., Liu, L., Li, C., Xue, X., Liang, X., *J. Colloid Interface Sci.* 2009, *337*, 420–426.

[10] Li, Y., Cheng, S., Dai, P., Liang, X., Ke, Y., *Chem. Commun.* 2009, *9*, 1085–1087.

[11] Xiao, Y., Tan, T. T. Y., Ng, S.-C., *Analyst* 2011, *136*, 1433–1439.

[12] Shen, Y., Smith, R. D., Unger, K. K., Kumar, D., Lubda, D., *Anal. Chem.* 2005, *77*, 6692–6701.

[13] Xiang, Y., Wu, N., Lippert, J. A., Lee, M. L., *Chromatographia* 2002, *55*, 399–403.

[14] Xiang, Y., Yan, B., McNeff, C. V., Carr, P. W., Lee, M. L., *J. Chromatogr. A* 2003, *1002*, 71–78.

[15] MacNair, J. E., Patel, K. D., Jorgenson, J. W., *Anal. Chem.* 1999, *71*, 700–708.

[16] MacNair, J. E., Lewis, K. C., Jorgenson, J. W., *Anal. Chem.* 1997, *69*, 983–989.

[17] Wang, Y., Ai, F., Ng, S.-C., Tan, T. T. Y., *J. Chromatogr. A* 2012, *1228*, 99–109.

[18] Thomas, A., Kohler, M., Schänzer, W., Kamber, M., Delahaut, P., Thevis, M., *Rapid Commun. Mass Spectrom.* 2009, *23*, 2669–2674.

[19] Keane, D. A., Hanrahan, J. P., Copley, M. P., Holmes, J. D., Morris, M. A., *J. Porous Mater.* 2010, *17*, 145–152.

[20] Gritti, F., Guiochon, G., *J. Chromatogr. A* 2010, *1217*, 1604–1615.

[21] Mallett, D. N., Ramírez-Molina, C., *J. Pharm. Biomed. Anal.* 2009, *49*, 100–107.

[22] Tylová, T., Kameník, Z., Flieger, M., Olšovská, J., *Chromatographia* 2011, *74*, 19–27.

[23] Fekete, S., Ganzler, K., Fekete, J., *J. Pharm. Biomed. Anal.* 2011, *54*, 482–490.

[24] Nilsson, C., Nilsson, S., *Electrophoresis* 2006, *27*, 76–83.

[25] Luedtke, S., Adam, T., vonDoehren, N., Unger, K. K., *J. Chromatogr. A* 2000, *887*, 339–346.

[26] Unger, K. K., Kumar, D., Grün, M., Büchel, G., Lüdtke, S., Adam, T., Schumacher, K., Renker, S., *J. Chromatogr. A* 2000, *892*, 47–55.

[27] Aturki, Z., Schmid, M. G., Chankvetadze, B., Fanali, S., *Electrophoresis* 2014, *35*, 3242–3249.

[28] Auditore, R., Santagati, N. A., Aturki, Z., Fanali, S., *Electrophoresis* 2013, *34*, 2593–2600.

[29] Domínguez-Vega, E., Crego, A. L., Lomsadze, K., Chankvetadze, B., Marina, M. L., *Electrophoresis* 2011, *32*, 2700–2707.

[30] Ai, F., Li, L., Ng, S.-C., Tan, T. T. Y., *J. Chromatogr. A* 2010, *1217*, 7502–7506.

[31] Li, L.-S., Wang, Y., James Young, D., Ng, S.-C., Tan, T. T. Y., *Electrophoresis* 2010, *31*, 378–387.

[32] Lin, B., Zheng, M. M., Ng, S. C., Feng, Y. Q., *Electrophoresis* 2007, *28*, 2771–2780.

[33] Stöber, W., Fink, A., Bohn, E., *J. Colloid Interface Sci.* 1968, *26*, 62–69.

[34] Vallet-Regí, M., Balas, F., *Open Biomed. Eng. J.* 2008, *2*, 1–9.

[35] Armstrong, D. W., *US-Patent* 1985, 4539399.

[36] Messina, A., Flieger, M., Bachechi, F., Sinibaldi, M., *J. Chromatogr. A* 2006, *1120*, 69–74.

[37] Ng, S.-C., Ong, T.-T., Fu, P., Ching, C.-B., *J. Chromatogr. A* 2002, *968*, 31–40.

[38] Wang, Y., Young, D. J., Tan, T. T. Y., Ng, S.-C., *J. Chromatogr. A* 2010, *1217*, 5103–5108.

[39] Berthod, A., Chang, C.-D., Armstrong, D. W., *Talanta* 1993, *40*, 1367–1373.

[40] McCalley, D. V., *J. Chromatogr. A* 2010, *1217*, 858–880.

[41] Lin, B., Shi, Z. G., Zhang, H. J., Ng, S. C., Feng, Y. Q., *Electrophoresis* 2006, *27*, 3057–3065.

Address：489 Songtao Road, C01, Zhangjiang High-tech Park, Pudong, Shanghai 201203, P.R. China
E-Mail：info@unimicrotech.com，lemonyu@unimicrotech.com
Website：www.unimicrotech.com

